Imaging Facial Signs of Neurophysiological Responses

Dvijesh Shastri, *Associate Member, IEEE*, Arcangelo Merla, *Member, IEEE*, Panagiotis Tsiamyrtzis, and Ioannis Pavlidis*, *Senior Member, IEEE*

***Abstract*—In the present paper, we introduce an integrated framework for detecting peripheral sympathetic responses through purely imaging means. The measurements are performed on three facial areas of sympathetic importance, that is, periorbital, supraorbital, and maxillary. To the best of our knowledge, this is the first time that the sympathetic importance of the maxillary area is analyzed. Because the imaging measurements are thermal in nature and are composed of multiple components of variable frequency (i.e., blood flow, sweat gland activation, and breathing), we chose wavelets as the image analysis framework. The measurements also carry substantial noise due to imperfections in tissue tracking and segmentation. The image analysis is grounded on galvanic skin response (GSR) signals, which are still considered the golden standard in peripheral neurophysiological and psychophysiological studies. The experimental results show that monitoring of the facial channels yields similar detecting power to GSR's. However, detailed quantification of the responses, although feasible in GSR through appropriate modeling, is quite difficult in the facial channels for the moment. Further improvements in facial tissue tracking and segmentation are bound to overcome this limitation. This paper opens a new research area that leads to unobtrusive screening technologies in neurophysiology and psychophysiology.**

***Index Terms*—Facial physiology, galvanic skin response (GSR), stress, thermal imaging, wavelets.**

I. Introduction

THE AUTONOMIC nervous system (ANS) and particularly its sympathetic division has been the object of intense study in neurophysiology and psychophysiology. The sympathetic division readies the body for a crisis that may require sudden, intense physical activity. It is a primal survival mechanism. Therefore, interest on methodologies that scrutinize sympathetic responses is well founded and has many applications.

When sympathetic activation occurs, an individual experiences many changes. Among others, these include increased activity in the cardiovascular and respiratory centers of the pons and medulla oblongata, leading to elevations in blood pressure, heart rate, breathing rate, and depth of respiration. These vital sign changes are mediated through adrenergic postganglionic fibers. Determination of sympathetic activation through vital sign monitoring is not always straightforward. Vital signs are often affected by pathophysiology and the time resolution of their sympathetic activation is limited by the long-lasting effect of norepinephrine release.

As an alternative, researchers focused their efforts on sympathetic manifestations effected through cholinergic postganglionic fibers. These fibers innervate sweat glands of the skin and the blood vessels to skeletal muscles and the brain. They provide a pathway to stimulating sweat gland secretion and selectively enhancing blood flow to muscles. Cholinergic mediation results in local physiological signs (versus vital signs), which are more descriptive (least affected by pathophysiology) and fast acting (fine time resolution).

In this context, electrodermal activity (EDA) has been the gold standard for peripheral monitoring of sympathetic responses. EDA is measured through the galvanic skin response (GSR), which is a simple and reproducible method for quantifying sweat gland activation. During arousal, the exposed part of the human body where sweat gland activation is considered to be the strongest is the palm. Therefore, the GSR sensor is attached to the palm or the fingers and the corresponding signal represents a change in the electrical properties of the palm's skin. Alternatively, EDA can be captured through a palm thermistor, which registers the full thermoregulatory phenomenon including changes both in blood flow and sweat gland activation.

In recent years, we have demonstrated that during arousal additional physiological signs materialize on the face. Specifically, we have shown that increased blood flow in the periorbital [1], [2] and supraorbital [3] areas are ubiquitous manifestations of stress. We have also developed a thermal imaging methodology to extract both the periorbital and supraorbital signals. This methodology has introduced a paradigm shift in peripheral neurophysiological and psychophysiological studies in more than one way as follows.

1) Contact-free 2-D sensing of easily accessible tissue (i.e., face) versus contact-probe 1-D sensing of less accessible tissue (e.g., palm or finger).
2) Motion effects are canceled to a degree by tissue tracking technology. This lessens the restrictions on the subject during experimentation.
3) Measurements are effected through computation and not electronic transduction.

In the present paper, we comparatively study facial and palm channels. The facial channels include overall thermoregulatory

Manuscript received February 6, 2008; revised May 29, 2008. First published August 15, 2008; current version published March 25, 2009. This work was supported by the National Science Foundation under Grant ISS-0414754, Grant ISS-0741581, and Instrumentation Grant CNS-0521527 to the Project "Interacting with Human Physiology." *Asterisk indicates corresponding author.*

D. Shastri is with the Computational Physiology Laboratory, University of Houston, Houston, TX 77204-0101 USA.

A. Merla is with the Department of Clinical Sciences and Bioimaging, University of Chieti-Pescara and Fondazione Università Gabriele d'Annunzio—Chieti, 66100 Chieti, Italy.

P. Tsiamyrtzis is with the Department of Statistics, Athens University of Economics and Business, Athens 10434, Greece.

*I. Pavlidis is with the Computational Physiology Laboratory, University of Houston, Houston, TX 77204-0101 USA (e-mail: ipavlidis@uh.edu).

Digital Object Identifier 10.1109/TBME.2008.2003265

responses in the periorbital, supraorbital, and maxillary regions, obtained through thermal imaging. The palm channels include sweat and thermal component responses obtained through GSR and thermistor sensors, respectively. The study focuses on a classic repeated arousal experiment. The main thesis of the paper is that thermoregulatory information of sympathetic importance on the palm is similar to the one manifested on the face. To test this hypothesis, first, we introduce a new modeling methodology to quantify the GSR signal and validate the arousal experiment. Then, we apply a wavelets analysis method for all channels (periorbital, supraorbital, maxillary, GSR, and thermistor). The results reveal tonic (baseline) and phasic (event related) affinity of the three imaging channels to the GSR and thermistor channels. We also demonstrate that from the maxillary signal, computation of breath function is feasible through multiresolution analysis. A unique result presented in this paper is evidence of concomitant sweat gland activationin the palm and maxillary areas. To the best of our knowledge, it is the first time that this maxillary thermoregulatory phenomenon is brought to the fore.

Out of our research is emerging the pivotal role of facial physiology in the manifestation of stress. It is the first time that this role emerges in all its facets and its redundancy to local signs in other parts of the body (i.e., palm) is demonstrated. It is also remarkable that sensing of peripheral sympathetic responses can now be accomplished through imaging means.

In the rest of the paper, we unveil our new imaging methodology for modeling and analyzing the facial sympathetic channels. Specifically, in Section II, we describe the method itself. In Section III, we report and discuss its experimental validation. In Section IV, we conclude the paper.

II. Methodology for Signal Modeling and Analysis

A. Modeling of GSR Signal

The first goal is to model the GSR signal and be able to draw inferences about the repeated arousal effect on each subject. Specifically, our modeling scheme needs to show that when individuals tend to habituate to the stimulation paradigm, GSR amplitudes tend to reduce, latencies tend to increase, while wave shapes tend to remain unaltered [4]. These well established and understood patterns of repeated arousals in normal subjects, if quantified here, will validate our experimental design and execution.

As we will discuss in the experimentation section (i.e., Section III), we stimulate the subjects with three auditory startles spaced at least 1 min apart. For this reason, we choose to split the GSR signal in three nonoverlapping segments:

1) S1: 2 s before the first startle until 2 s before the second startle;
2) S2: End of $S1$ to 2 s before the third startle;
3) S3: End of $S2$ to end of the experiment.

We divide each of the segments S1, S2, and S3 into three subsegments:

1) LS: The left subsegment, which spans from the beginning of the segment till the maximum value (shortly after startle).

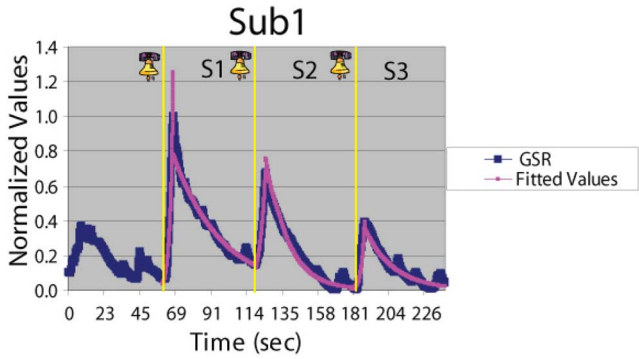

Fig. 1. GSR segments S1, S2, and S3 along with the fitted Laplace values for subject Sub1. The stimuli occurrences have been marked appropriately.

2) RS: The right subsegment, which spans from the maximum value till the end of the segment.
3) LSOS: The left stimulus onset subsegment, which starts at the time of the startle and lasts until the maximum value is reached, is a portion of the LS and is useful in estimating the habituation effect.

The GSR signal around the stimulus is formed by the charging and discharging of an *RC* circuit, which closes on the palm skin during emotional sweat gland activation. Charging corresponds to arousal (LS) and is characterized by an exponential increase. Discharging corresponds to arousal waning (RS) and it follows an exponential decay. For this reason, we choose the Laplace distribution to model the GSR signal. The probability density function is given by

$$f(t \mid \mu, \beta) = \frac{1}{2\beta} \exp\left(-\frac{|t-\mu|}{\beta}\right) \tag{1}$$

where μ denotes the mean time parameter, while $\beta > 0$ is the scale parameter.

Although the GSR signal is not symmetric around the local maximum value, the Laplace distribution is. This led us to model separately the LS and RS for every segment (see Fig. 1). For LS, we fit a truncated Laplace distribution, where the μ parameter is assumed to be known (location of the maximum) and the distribution is censored to the right of the maximum. Similarly, for RS, we use a truncated Laplace distribution, where the values at the left of the maximum are censored. The goal then is to estimate the scale parameters of the left and right distributions (i.e., β_L and β_R). This estimation is done through the ordinary least squares (OLS) method.

For LS, where $t \leq \mu$, we have

$$y = f(t) = \frac{1}{2\beta_L} \exp\left(-\frac{\mu - t}{\beta_L}\right)$$
$$\Rightarrow \ln(y) = \left[-\frac{\mu}{\beta_L} - \ln(2\beta_L)\right] + \frac{1}{\beta_L} t \tag{2}$$

so that time t and logarithmic scale $\ln(y)$ are linearly related. We use OLS to estimate the slope, whose inverse is the parameter of interest β_L.

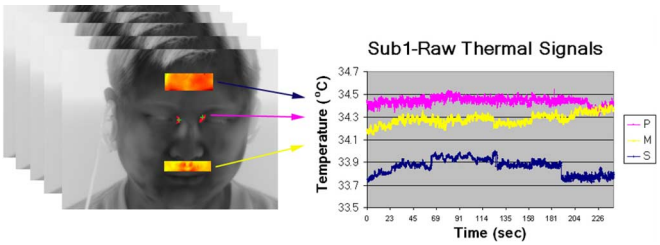

Fig. 2. Periorbital, supraorbital, and maxillary regions of interest. The periorbital measurement is strictly localized on the thermal footprints of the facial artery.

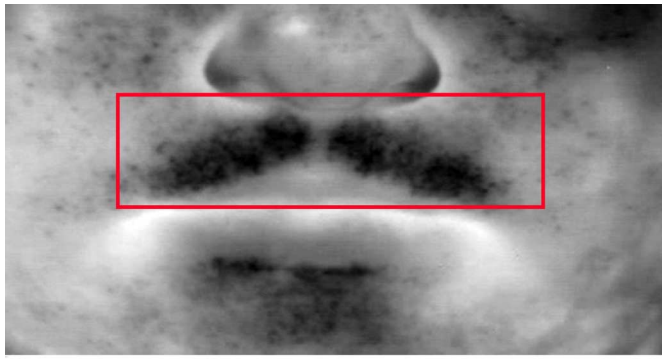

Fig. 3. Thermal facial image of high spatial resolution. The high concentration of perspiration pores in the maxillary area is evident.

For RS, where $t \geq \mu$, we have

$$y = f(t) = \frac{1}{2\beta_R} \exp\left(-\frac{t-\mu}{\beta_R}\right)$$

$$\Rightarrow \ln(y) = \left[\frac{\mu}{\beta_R} - \ln(2\beta_R)\right] - \frac{1}{\beta_R} t \tag{3}$$

so that time t and logarithmic scale $\ln(y)$ are linearly related. We use OLS to estimate the slope, whose negative inverse is the parameter of interest β_R.

For LSOS, we apply linear fitting, as these subsegments are nearly impulsive.

B. Wavelets Analysis of Sympathetic Signals

We extract thermal signals from three facial areas: periorbital, supraorbital, and maxillary. In all three cases, the regions of interest are tracked using the coalitional tracking method, as reported in [5]. In the periorbital area, the extracted signal is formed from the evolution of the mean thermal footprint of the facial arteriovenous complex. This footprint is segmented via a fuzzy segmentation algorithm, which is seeded in the initial frame with two points in the inner orbital areas (see Fig. 2). On each subsequent frame, the seeds are adjusted with help from the coalitional tracker. In the supraorbital area, the extracted signal is formed from the evolution of the mean thermal footprint of the entire region of interest. In the maxillary area, the extracted signal is formed from the evolution of the mean thermal footprint of the entire region of interest.

The periorbital thermal signal is a correlate of the blood supply to the orbital muscle [1], [2]. The supraorbital thermal signal is a correlate of the blood supply to the corrugator muscle [3]. The maxillary thermal signal is a correlate of the blood perfusion in the respective area. The last two signals may be modulated from the activation of sweat glands in the respective areas. This modulation appears to be heavier in the maxillary area, partly due to higher concentration of perspiration pores (see Fig. 3). Finally, the maxillary signal is periodically modulated from the thermal effect of breathing, due to the proximity of nostrils.

Concomitantly with the three facial imaging signals, we extract palm perspiratory and thermal signals through GSR and thermistor sensors, respectively. We also extract the breathing signal through a piezo-respiratory belt transducer. All probe signals (GSR, palm thermistor, and respiratory belt) are synchronized with the thermal imager through an electronic circuit.

The stress content of the GSR signal has been documented in the literature exhaustively [4], [6], [7]. We have also investigated the stress content of the periorbital and supraorbital channels in a number of publications [1]–[3]. In this paper, we introduce and characterize the maxillary signal as the facial equivalent of the palm signals. To study the maxillary signal in comparison with the ground-truth palm signals as well as the other facial signals, we use a multiresolution wavelets approach. This approach is also conducive to understanding the thermal effect of breathing in the maxillary measurement.

Specifically, we consider that all signals if they are of sympathetic importance have either a strong phasic or tonic component [8]. The phasic component should be at a scale that matches the interstimulus interval of the experiment, while the tonic component will reside at an even higher scale that spans the entire experimental timeline. Any strong extraneous modulation (e.g., breathing) in some signals should be evident in a lower scale (i.e., higher frequency), far away from the phasic and tonic scales.

Our goal is to analyze the thermal and GSR signals at different frequency scales but without loss of time information. Since the signals are nonstationary in nature, we select the wavelet transformation over the FFT for signal analysis. To quantify the contribution of phasic, tonic, and other components in the signals, we first normalize all the signals

$$S_{\text{norm}} = \frac{S - \text{Min}(S)}{\text{Max}(S) - \text{Min}(S)} \tag{4}$$

where S is signal to be normalized. Normalization is essential in wavelet analysis because wavelet energy computed on normalized signals exposes detailed information, specifically at the lower scales (see Fig. 4).

Next, we extend the signals beyond the boundary limits before computing wavelet coefficients. Convolution of a wavelet with a finite-length signal looks for data points beyond the signal end points. As there are no data points beyond the signal end points, this introduces an error in the wavelet energy computation, which is known as the border discontinuity error. The border discontinuity error leads to wrong local and global maxima in wavelet energy curves (see Fig. 5). The purpose of the signal

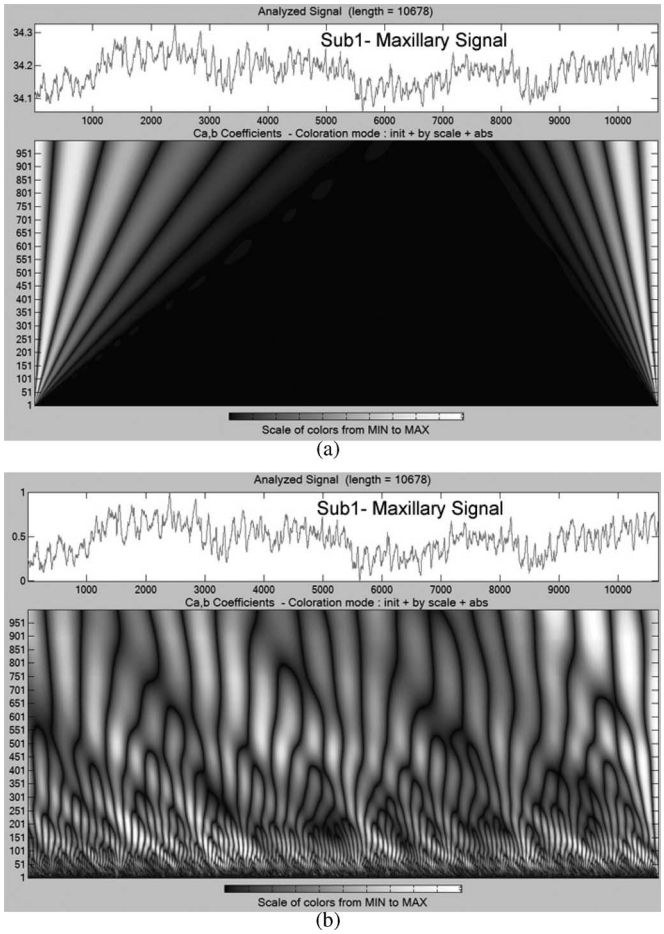

Fig. 4. Wavelet energy plots for subject Sub1: (a) without signal normalization and (b) with signal normalization. Wavelet energy plot of a normalized signal reveals detailed information at the lower scales.

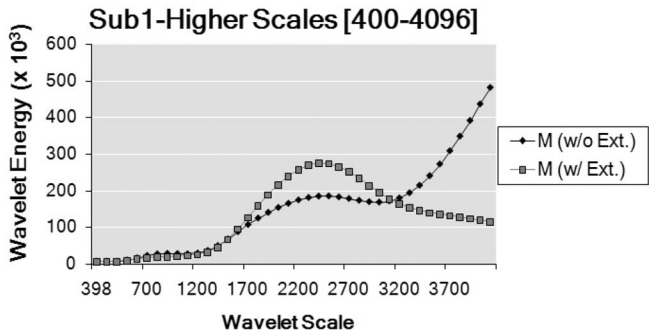

Fig. 5. Wavelet energy graph for subject Sub1. The black curve corresponds to a signal without extension, while the gray energy curve corresponds to a signal with extension. The latter reveals the true global maximum in this energy graph.

extension is to define data points beyond the signal boundary. There are many ways to extend the finite-length signal. Among them, zero-padding, wraparound, and symmetric extension are popular in the image and signal analysis communities. As our signals are nonstationary in nature, we select the symmetric extension technique. Selecting an appropriate signal extension length is also very important in the wavelet energy computation. We apply three different extension lengths, $2N$, N, and $N/2$, and for each signal, we choose the one that has the minimal border discontinuity error in the wavelet energy computation.

To quantify the contribution of phasic, tonic, and other components in the preprocessed signals, we apply a continuous wavelet transform (CWT) with a Daubechies-10 mother wavelet. Finally, we compute the energy of each signal in all scales. The energy curves feature global and local maxima. We analyze these maxima to understand if they correspond to phasic or tonic responses. We also compare their relative contributions in each signal. For intervening phenomena for which we have ground truth (e.g., breathing), we perform a comparative evaluation to verify the source of the wavelet component beyond doubt.

Out of this image analysis, an intriguing picture of the facial physiology of stress is emerging, tied to a trustworthy channel that served well in research and practice for many years (i.e., GSR) and from an experiment whose validity has been verified through the modeling approach described in Section II-A.

III. Experimentation and Discussion

We used a high-quality thermal imaging (TI) system for data collection. The centerpiece of the TI system is a ThermoVision SC6000 midwave infrared (MWIR) camera [9] (NEDT = 0.025 °C). We recorded ten thermal clips from the faces of ten subjects while resting in an armchair. Concomitantly, we recorded ground-truth GSR, palm thermistor, and piezorespiratory signals with the PowerLab 8/30, ML870 data acquisition system [10].

The dataset included subjects of both genders, different races, and with varying physical characteristics. Exclusion criteria were the presence of any overt peripheral neuropathy or psychophysiological disorder. The subjects were asked to abstain from consuming vasomotor substances (e.g., caffeine and nicotine) for at least 3 h prior to participating in the experiment. All participants signed the informed consent form and the study protocol was approved by the Univesity of Houston Institutional Review Board.

The experiment was conducted in a quiet room where only two persons were present, the subject and the experiment conductor. The room lights were dimmed in order to allow the subject to relax. The subject was placed 9 ft away from the thermal camera. After all, the ground-truth electrodes were attached to the subject's body, the subject was asked to relax for 10 min before the experiment began. This helped to reduce the effects of other stress factors that the subject may have carried in from previous events. During the experiment, the subject focused on the simple mental task of counting circles that appeared on a monitor. The subject's physiological activity was measured through thermal imaging and contact sensors (see Fig. 6). The experiment lasted 4 min. After the first minute, an auditory startle was delivered, and after that, two more were delivered, spaced 1 min apart. All stimuli were chosen to be natural startle sounds that people encounter in real life. Specifically, the first and third stimuli were glass breakage sounds. The second stimulus was phone ring. We chose the second stimulus to be

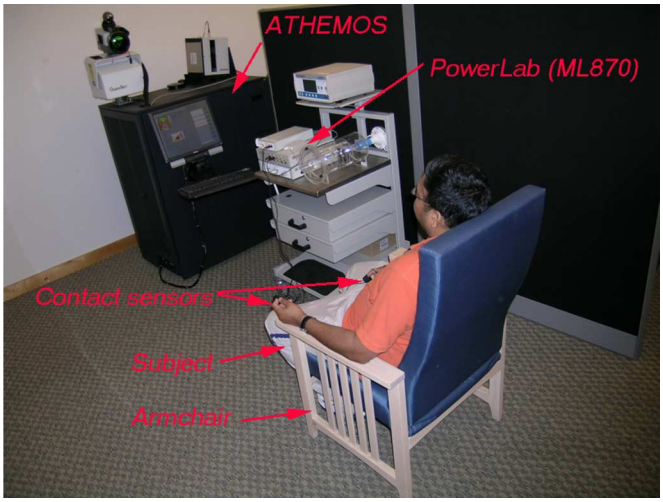

Fig. 6. Experimental setup; subject, imaging and ground truthing clinical equipment.

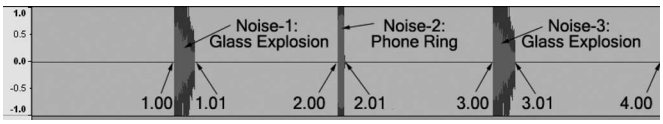

Fig. 7. Experimental timeline; the auditory startle sound was delivered after every minute.

different than the other two to raise the habituation threshold. The experiment ended 1 min after the delivery of the third startle (see Fig. 7). During the data collection procedures, the experimenter was out of the subject's field of view to avoid creating distraction.

A. GSR Results

We applied the modeling methodology detailed in Section II-A to each segment of every GSR waveform. Therefore, we had three segments (S1, S2, S3) $\times$ 3 subsegments (LS, RS, LSOS) $\times$ 10 subjects $=$ 90 cases for which we needed to estimate the scale parameter β (Laplace fitting for LS and RS) or the slope (linear fitting for LSOS). The results are shown in Table I and elicit the following conclusions.

1) For almost all stimuli (S1, S2, and S3), LS has a much smaller scale parameter than RS indicating that the phenomenon causes a steep increase and then decays at a much lower rate.
2) Comparing the LS parts of S1, S2, and S3, within the same subject, we observe that usually the 1st stimulus causes the steepest increase, and as we move to subsequent stimuli, the response is less steep (i.e., the β_L parameter is increasing).
3) Comparing the RS parts of S1, S2, and S3, within the same subject, we observe that usually the subject recovers slowly after the 1st stimulus (i.e., it has a high β_R parameter). Recovery from subsequent stimuli is becoming faster (smaller β_R parameter).
4) Comparing the LSOS parts of S1, S2, and S3, within the same subject, we observe that usually the estimated (positive) slope of the linear regression is decreasing as we move from S1 to S2 to S3 (habituation).

These conclusions are in accordance with the expected behavior of normal subjects, and therefore, our experiment is valid.

B. Comparative Wavelets Analysis Results

We have applied the wavelets analysis methodology detailed in Section II-B for all six sympathetic signals from all ten subjects. Fig. 8 shows the wavelet energy curves in lower and higher scales of subject Sub1. In lower scales (i.e., 50–250), the piezorespiratory signal (Brt) appears to have a dominant component, as it is manifested by the high bell-shaped bulge. This is in accordance with its expected function. The second most prominent component is featured by the maxillary signal (M). This verifies our hypothesis of breathing modulation for this signal, as it is sampled in proximity to the nostrils. Fig. 9 is a superimposition of the wavelet components that correspond to the local energy maxima of the Brt and M for subject Sub1. There is a slight, but consistent phase shift due to the fact that the Brt signal is sampled around the chest while the M signal in the vicinity of the nostrils. Other than that, the periodicity of the signals matches beat for beat. Similar results are produced for the other subjects.

In higher scales, (i.e., 1000–3000), the GSR signal appears to have a dominant component, as it is manifested by the high bell-shaped bulge [see Fig. 8(b)]. This is the phasic component as the scale is about $1/3$ of the total scale and matches the period of the repeated stimuli in our experiment. The strong presence of a phasic component in the GSR signal is consistent with its nature. The fascinating result here is the almost equally strong phasic component in the maxillary signal (M). This is consistent with our hypothesis of strong sweat gland activation in the maxillary area concomitant to the palm area. Other facial signals (i.e., periorbital-P and supraorbital-S) also have significant but relatively weaker phasic components, which verifies their sympathetic relevance.

The phasic components of the thermal and GSR signals illustrate another fascinating result (see Fig. 10). The phasic component of the periorbital signal (P) has a 180° phase shift with respect to the phasic component of the maxillary signal (M) but is in phase with the phasic component of the GSR signal. The periorbital signal is associated with the blood supply to the orbital muscle, which elevates the temperature of the periorbital region during stimulation. The maxillary signal, on the other hand, is heavily modulated by sweat gland activity during stimulation, which decreases the temperature of the maxillary region. Therefore, an inverse relation exists between the phasic components of the periorbital and maxillary signals. This inverse relation may be difficult to visualize through raw data, but it becomes clear through wavelet analysis. The GSR signal, which represents skin conductivity, exhibits a steep increase during stimulation while the facial temperature changes relatively slowly. However, although the GSR and periorbital signals are changing at different speeds around the stimuli, their changes

TABLE I
ESTIMATED β PARAMETERS FOR LS AND RS LAPLACE DISTRIBUTIONS ALONG WITH LINEAR REGRESSION SLOPE ESTIMATES OF LSOS

	Sub1	Sub2	Sub3	Sub4	Sub5	Sub6	Sub7	Sub8	Sub9	Sub10
$S1$-LS	2.18	2.68	1.70	1.94	7.50	14.54	4.79	25.39	4.50	3.87
$S1$-$LSOS$	0.20	0.10	0.15	0.14	0.13	0.05	0.06	0.05	0.08	0.12
$S1$-RS	30.40	33.90	27.11	40.89	36.88	82.50	151.47	38.76	68.08	25.24
$S2$-LS	3.75	3.04	1.77	8.49	5.69	26.16	7.89	13.13	8.29	9.37
$S2$-$LSOS$	0.11	0.07	0.13	0.08	0.12	0.03	0.10	0.04	0.10	0.11
$S2$-RS	13.39	29.46	34.11	62.67	22.46	53.43	44.81	20.71	61.65	30.69
$S3$-LS	1.91	2.51	2.30	10.13	2.51	62.46	15.09	2.28	10.63	5.49
$S3$-$LSOS$	0.09	0.09	0.12	0.06	0.12	0.01	0.03	0.08	0.07	0.08
$S3$-RS	17.93	11.36	34.25	66.67	19.12	31.53	81.62	108.44	25.21	13.44

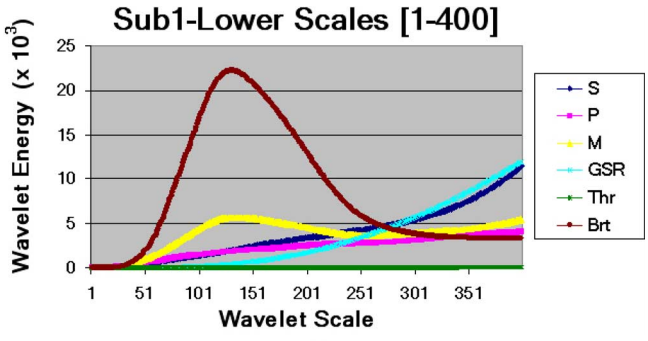

(a)

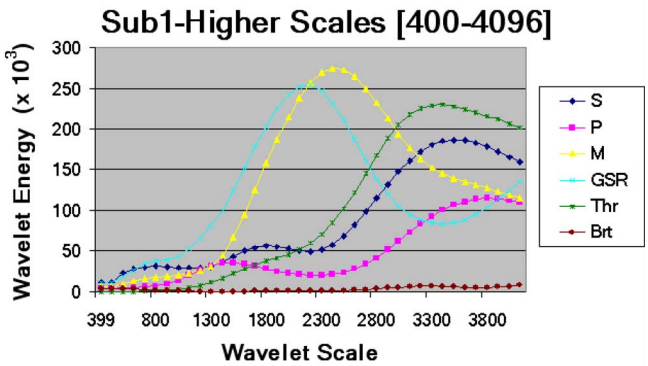

(b)

Fig. 8. Wavelet energy curves of subject Sub1 for all six sympathetic channels in (a) lower and (b) higher scales.

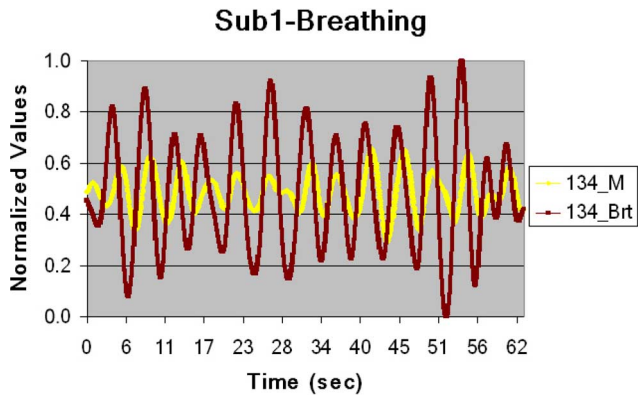

Fig. 9. Wavelet components of the Brt and M signals that correspond to the respective lower scale energy maxima.

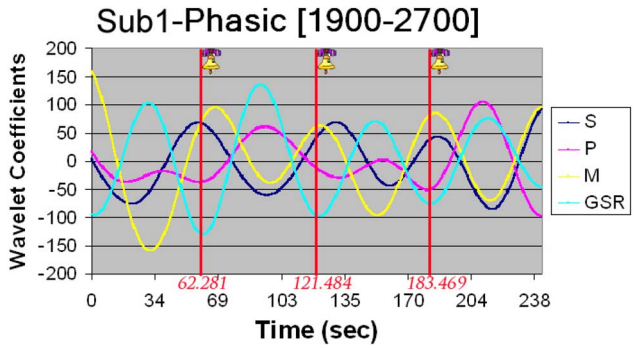

Fig. 10. Phasic components of thermal and GSR signals for subject Sub1. Phase shift of 180° is observed between the phasic component of maxillary and periorbital signals. The phasic component of the periorbital signal is in phase with the GSR signal.

are in phase. The wavelet analysis illustrates this relationship very clearly at the phasic level.

The tonic components of the signals reside at the highest scales (3300–4000) that span almost the entire timeline. It is worth noting that the GSR signal has the smallest tonic component of all sympathetic channels. This is consistent with the nature of the GSR channel. The maxillary signal (M), which is its facial equivalent, has a much stronger tonic component. In contrast to the GSR signal, the maxillary signal contains not only local sweat gland activation information, but also thermal information related to changes in local blood perfusion. In this sense, the maxillary signal (M) is probably closer to the palm thermistor (Thr) signal.

In general, adrenergic and cholinergic signal components reside in nonoverlapping scales, which makes the adopted multiresolution approach an ideal analysis tool. A case in point can be made if we remove the breathing component from the raw maxillary signal [see Fig. 11(a)] and recompute the wavelet energy. The curve no longer shows the breathing bulge at lower scales [see Fig. 11(b)].

The picture emerging from the analysis of the wavelet energy curves for subject Sub1 remains relevant for all the other nine subjects in our dataset. Fig. 12 shows the mean energy of tonic, phasic, and breathing components of the various sympathetic channels for the entire dataset. All the conclusions extracted through the example of subject Sub1 still apply for the mean subject.

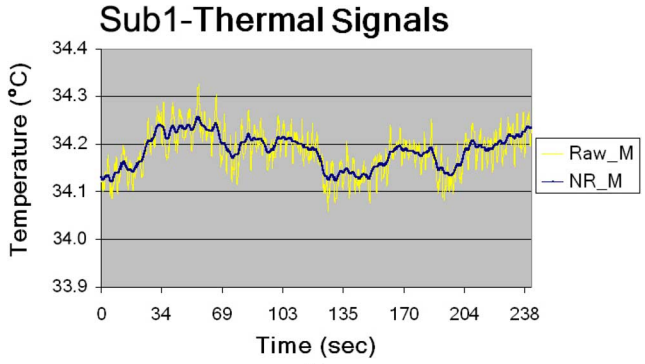

(a)

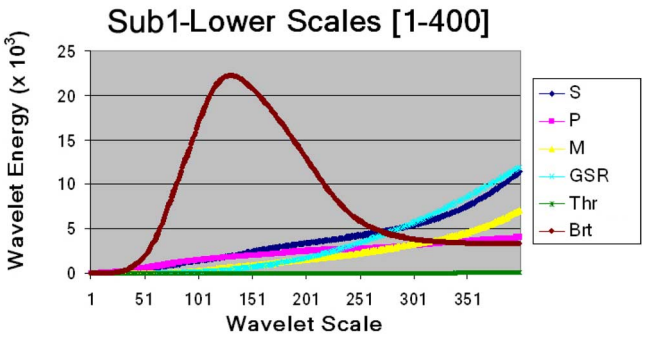

(b)

Fig. 11. (a) Maxillary signal in raw (Raw_M) and noise reduced (NR_M) forms. Noise reduction amounts to the removal of the breathing component. (b) Wavelet energy curves at lower scales. The wavelet energy curve of the maxillary channel after removing the breathing component does not feature a bulge at lower scales.

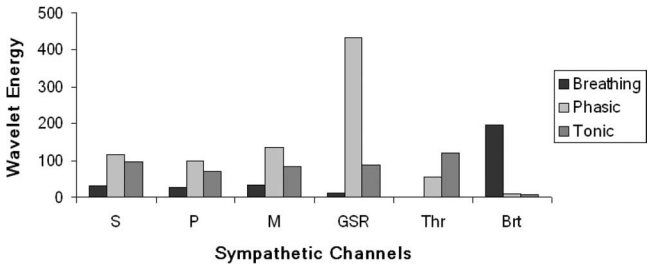

Fig. 12. Mean tonic, phasic, and breathing energy components for the various sympathetic channels.

IV. Conclusion

The wavelet energy analysis demonstrates quantitatively that facial sympathetic channels can be used to detect arousal. Specifically, the novel maxillary channel (M) has enough information content to localize sympathetic responses almost as well as the GSR channel. However, as we discussed in Section II-A, appropriate GSR modeling can enable quantification of important subtleties, like habituation. Unfortunately, the facial signals do not have the almost ideal quality of the raw GSR signal and direct modeling is difficult [see Fig. 13(a)]. The presence of multiple contributing thermal factors (e.g., blood flow, sweat gland activation, and breathing), as well as significant noise from tracking and segmentation imperfections renders modeling of the raw facial signals hard. In this context,

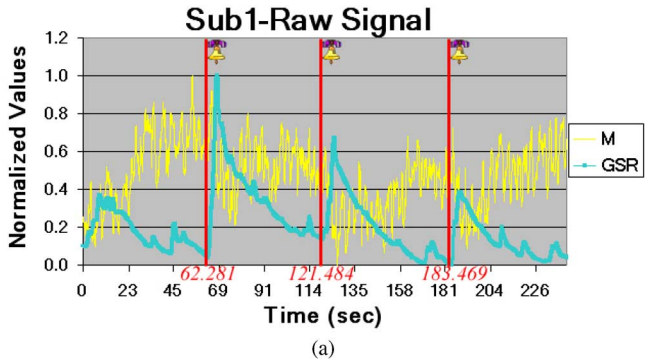

(a)

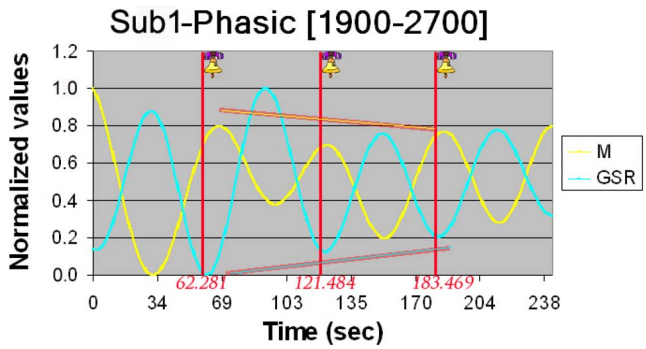

(b)

Fig. 13. (a) Raw GSR and maxillary (M) signals for subject Sub1. (b) The corresponding phasic wavelets with the enveloping waveguides. The occurrences of the stimuli are marked by the three vertical lines.

wavelet analysis provides a sound way to isolate the various components and reduce the noise content of the facial signals. The question then is if detailed arousal quantification, such as the one achieved through Laplace modeling for GSR, can be achieved through wavelet analysis for the facial channels. Fig. 13(b) demonstrates the phasic wavelets of the GSR and periorbital (P) signals for subject Sub1. The two channels have almost identical response timing and overall trend. Habituation in the GSR signal can be computed through the enveloping waveguides. The same can be accomplished for the periorbital wavelet. Still, the deleterious effect of residual noise in the periorbital signal is evident, which for the moment allows only trend computation and precludes precise estimation that can scale up in the dataset. Our ongoing research aims to improve the quality of the facial signals through advancements in tissue segmentation and tracking technology. Then, detailed annotation of phasic responses (not just detection) will be absolutely feasible for all three facial channels.

Acknowledgment

Research activity involving human subjects has been reviewed and approved by the University of Houston Committee for the Protection of Human Subjects. We would like to thank all the volunteer subjects who participated in our test population. We would also like to thank Dr. E. Glinert from the National Science Foundation (NSF) for his support and encouragement in this nascent technology effort. This material is based

upon work supported by the National Science Foundation under Grant ISS-0414754 and ISS-0741581, entitled "Interacting with Human Physiology." The equipment used in this research was also supported by NSF under instrumentation Grant CNS-0521527. Any opinions, findings, and conclusions or recommendations expressed in this material are those of the author(s) and do not necessarily reflect the views of the National Science Foundation.

REFERENCES

[1] J. Levine, I. Pavlidis, and M. Cooper, "The face of fear," *Lancet*, vol. 357, no. 9270, p. 1757, Jun. 2001.
[2] I. Pavlidis, N. L. Eberhardt, and J. Levine, "Human behavior: Seeing through the face of deception," *Nature*, vol. 415, no. 6867, p. 35, Jan. 2002.
[3] C. Puri, L. Olson, I. Pavlidis, and J. Starren, "Stresscam: Non-contact measurement of users' emotional states through thermal imaging," in *Proc. 2005 ACM Conf. Hum. Factors Comput. Syst. (CHI)*, Portland, OR, Apr. 2–5, 2005, pp. 1725–1728.
[4] A. Uncini, S. Pullman, R. Lovelace, and D. Gambi, "The sympathetic skin response: Normal values, elucidation of afferent components and application limits," *J. Neurosci.*, vol. 87, pp. 299–306, 1988.
[5] J. Dowdall, I. T. Pavlidis, and P. Tsiamyrtzis, "Coalitional tracking," *Comput. Vis. Image Understand.*, vol. 106, no. 2–3, pp. 205–219, May 2007.
[6] M. Baba, Y. Watahiki, M. Matsunaga, and K. Takebe, "Sympathetic skin response in healthy man," *Electromyogr. Clin. Neurophysiol.*, vol. 28, pp. 277–283, 1988.
[7] B. Elie and P. Guiheneuc, "Sympathetic skin response: Normal results in different experimental conditions," *Electroencephalogr. Clin. Neurophysiol.*, vol. 76, no. 3, pp. 258–267, 1990.
[8] C. L. Lim, C. Renniea, R. Barry, H. Bahramali, I. Lazzaro, B. Manor, and E. Gordon, "Decomposing skin conductance into tonic and phasic components," *Int. J. Psychophysiol.*, vol. 25, pp. 97–109, 1997.
[9] FLIR Systems, Goleta, CA [Online]. Available: http://www.flir.com
[10] ADInstruments, Colorado Springs, CO [Online]. Available: http://www.adinstruments.com

Dvijesh Shastri (A'08) received the B.E. degree in electrical engineering from Sardar Patel University, Vallabh Vidyanagar, Gujarat, India, in 1997, the M.S. degree in computer science from Wright State University, Dayton, OH, in 2001, and the Ph.D. degree in computer science from the University of Houston, Houston, TX, in 2007.

He is currently a Research Assistant Professor at the Computational Physiology Laboratory, University of Houston. His current research interests include image/signal processing, computer vision, pattern recognition/classification, and biometrics.

Arcangelo Merla (M'07) received the M.S. (Laurea) degree in physics from the University of Bologna, Bologna, Italy, and the Ph.D. degee in advanced biomedical technologies and bioimaging from the University of Chieti, Chieti, Italy.

He had joined the Faculty of Clinical Sciences and Bioimaging, School of Medicine, University of Chieti, as of August 2002. Currently, he is the Director of the Functional Infrared Imaging Laboratory, Institute of Advanced Biomedical Technologies, University G. DAnnunzio, Chieti—Pescara, Italy, and a Visiting Assistant Professor at the Computational Physiology Laboratory, University of Houston, Houston, TX. He has published extensively in biomedical journals and refereed conference proceedings over the past years in the area of biomedical imaging and modeling, with special emphasis on infrared imaging and its biomedical applications.

Panagiotis Tsiamyrtzis received the B.S. degree in mathematics from the Department of Mathematics, Aristotle University of Thessaloniki, Thessaloniki, Greece, in 1994, and the M.S. and Ph.D. degrees in statistics from the School of Statistics, University of Minnesota, Minneapolis, in 1997 and 2000, respectively, where he served as a Visiting Faculty Member in Fall 2000.

In 2004, he joined the Department of Statistics, Athens University of Economics and Business, Athens, Greece, where he is currently a Lecturer. As of 2007 he is also Adjunct Assistant Professor at the Department of Computer Science, University of Houston. His current research interests include computer vision, statistical process control, and applications of Bayesian statistics.

Dr. Tsiamyrtzis was the recipient of the Best Student Paper Award and Best Contributed Paper in the 2000 Joint Statistical Meetings of the Risk Analysis Section of the American Statistical Association. He also received the Best Talk Award in the 2007 Annual Conference of the European Network for Business and Industrial Statistics.

Ioannis Pavlidis (S'85–M'87–SM'00) is the Eckhard Pfeiffer Professor of computer science and Director of the Computational Physiology Laboratory, University of Houston, Houston, TX. He is a Fulbright Fellow. He is well known for his work on stress quantification, which appeared in *Nature* and *Lancet*, and received worldwide scientific and media attention. He is the author or coauthor of many journal articles and books on the topics of computational physiology, computational psychology, computer vision, and pattern recognition.

Prof. Pavlidis has also established several well-known IEEE Conferences and Workshops, among them the IEEE Advanced Video and Signal Based Surveillance (AVSS) Conference.